

Spectroscopy and large scale wave functions

Qi-Zhou Chen,^a Shuo-Hong Guo,^a, Xiang-Qian Luo,^b and Antonio J. Segui-Santonja^c

^a *CCAST (World Laboratory), P.O. Box 8730, Beijing 100080, China
and Department of Physics, Zhongshan University, Guangzhou 510275, China*

^b *HLRZ, Forschungszentrum, D-52425 Jülich, Germany
and Deutsches Elektronen-Synchrotron DESY, D-22603 Hamburg, Germany*

^c *Departamento de Física Teórica, Universidad de Zaragoza, 50009 Zaragoza, Spain*

Abstract

We discuss the relevance of long wavelength excitations for the low energy spectrum of QCD, and try to develop an efficient method for solving the Schrödinger equation, and for extracting the glueball masses and long wavelength functions of the ground and excited states. Some technical problems appearing in the calculations of SU(3) gauge theory are discussed.

QCD in the pure gauge sector possesses a nontrivial vacuum structure and bound states called glueballs. Solving the Schrödinger equation in the Hamiltonian formulation can directly provide not only the glueball masses from the eigenvalues, but also the profiles, i.e., the wave functions for the ground state and excited states.

Strictly speaking, the continuum physics should be extracted in the asymptotic scaling region predicted by the renormalization group equation. In [1, 2, 3, 4, 5], we developed an efficient eigenvalue equation method with some new truncation schemes which preserve the continuum limit. This is an essential step towards the scaling.

Our starting point is to obtain the long wavelength wave functions of the ground and excited states. The philosophy is to keep the correct long wavelength limit during the truncation. The low energy spectrum originates mainly from the long wavelength excitations. This is because the size or the Compton length of a glueball, which is usually of the same order as that of a hadron or the lattice size, should be much greater than the lattice spacing a . It is worth mentioning that the confinement of gluons or static quarks is closely related to the long wavelength structure of the vacuum. For the long wavelength configurations U ,

the ground state in the continuum [6] is

$$|\Omega\rangle = \exp\left[-\frac{\mu_0}{e^2} \int d^{D-1}x \operatorname{tr} \mathcal{F}^2 - \frac{\mu_2}{e^6} \int d^{D-1}x \operatorname{tr} (\mathcal{D}\mathcal{F})^2\right], \quad (1)$$

with e being the renormalized coupling, \mathcal{F} the field strength tensor and \mathcal{D} the covariant derivative.

Our method is as follows. The ground state

$$|\Omega\rangle = \exp[R(U)]|0\rangle \quad (2)$$

with energy ϵ_Ω of the Hamiltonian H has to satisfy the Schrödinger equation $H|\Omega\rangle = \epsilon_\Omega|\Omega\rangle$, which results in

$$\begin{aligned} & \sum_l \{[E_l, [E_l, R(U)]] + [E_l, R(U)][E_l, R(U)]\} \\ & - \frac{2}{g^4} \sum_p \operatorname{tr}(U_p + U_p^\dagger) = \frac{2a}{g^2} \epsilon_\Omega. \end{aligned} \quad (3)$$

This equation can be solved by a systematic method [1, 2, 3, 4, 5], in which $R(U)$ is expanded in order of graphs $G_{n,i}$, i.e.,

$$R(U) = \sum_n R_n(U) = \sum_{n,i} C_{n,i} G_{n,i}(U), \quad (4)$$

with n being the order of the graphs defined as the number of plaquettes involved. Then the N th order truncated eigenvalue equation is

$$\begin{aligned} & \sum_l \{[E_l, [E_l, \sum_n R_n(U)]] \\ & + \sum_{n_1+n_2 \leq N} [E_l, R_{n_1}(U)][E_l, R_{n_2}(U)]\} \\ & - \frac{2}{g^4} \sum_p \operatorname{tr}(U_p + U_p^\dagger) = \frac{2a}{g^2} \epsilon_\Omega, \end{aligned} \quad (5)$$

from which the coefficients $C_{n,i}$ are determined. Similar equation for the glueball mass and its wave function can be derived [4].

Only the second term generates new or higher order graphs (of order $n_1 + n_2$), influencing the choice of independent graphs. The essential feature of our truncation scheme, which differs sufficiently from the scheme in [7], is in the treatment of this second term. It has been generally proven [1] that in the long wavelength limit this term should behave as

$$[E_l, R_{n_1}(U)][E_l, R_{n_2}(U)] \propto a^6 \operatorname{tr}(\mathcal{D}\mathcal{F}_{\mu,\nu})^2. \quad (6)$$

To preserve this correct limit, when the equation (5) is truncated to the N th order all the graphs created by $[E_l, R_{n_1}(U)][E_l, R_{n_2}(U)]$ for $n_1 + n_2 \leq N$ must be considered. In this method, no group integration is necessary, and independent graphs can be obtained systematically [3, 4], which can be suitably chosen for more rapid convergence to the continuum limit.

When the eigenvalue equation is truncated at a finite order, some ambiguity appears, as mentioned in [3, 8]. For a non-abelian gauge theory, the unimodular condition induces the mixing of a graph with not only the same order, but also different orders. Therefore, the definition of the order of a graph and the choice of independent graphs are not unique. In the infinite order limit, different prescriptions should give identical results. At low orders, this is not necessarily the case. Then a question arises: which classification scheme works more efficiently and converges more rapidly to the continuum limit? (In numerical simulation on a finite lattice, there is analogously a problem of choosing better operators or wave functions).

In $SU(2)$ gauge group, $\operatorname{Tr}U_p = \operatorname{Tr}U_p^\dagger$ and all loops with crossing can be transformed into loops without crossing. The complication of the $SU(3)$ group, however, is that not all the disconnected graphs can be transformed to the connected ones. Any group element A of $SU(3)$ has to satisfy the following condition

$$A_{i_1 j_1} A_{i_2 j_2} A_{i_3 j_3} \epsilon_{j_1 j_2 j_3} = \epsilon_{i_1 i_2 i_3}, \quad (7)$$

where a summation over the repeated indices is implied. We rewrite this condition as

$$\begin{aligned} 2(A^\dagger)_{ij} &= 2(A^2)_{ij} - 2A_{ij}\operatorname{tr}A \\ &+ [(\operatorname{tr}A)^2 - \operatorname{tr}(A^2)]\delta_{ij}, \end{aligned} \quad (8)$$

or

$$\begin{aligned} 2\delta_{ij} &= 2(A^3)_{ij} - 2(A^2)_{ij}\operatorname{tr}A \\ &+ [(\operatorname{tr}A)^2 - \operatorname{tr}(A^2)]A_{ij}, \end{aligned} \quad (9)$$

from which the relations among different graphs can be established. One sees that not only graphs of the same order, but also graphs of different orders mix, so that the classification becomes rather involved.

In [1, 2], the disconnected graphs were taken as independent graphs. We realize that this is not the most efficient way, because the disconnected graphs have large overlapping with graphs of lower orders in the weak coupling region. Indeed, the results in [2] showed that such a choice was not so economical. Alternatively, the connected graphs represent more coherence and have less mixing with lower order graphs. The superiority of the connected scheme over the disconnected one has also been shown in [8] for a (2+1)-dimensional SU(2) model. This is why for a more realistic gauge group SU(3), we try our best to transform [3] the disconnected graphs to the connected ones.

The coefficients μ_0 and μ_2 in (1) should be constants in the weak coupling limit $g \rightarrow 0$ or $\beta = 6/g^2 \rightarrow \infty$ as required by the renormalizability of the theory. Figure 1 shows the third order results for QCD₃ from the strong coupling expansion and the truncated eigenvalue equation. They are consistent in the strong coupling region. For larger β , it is not surprising that the strong coupling expansion method no longer works. It is usually hoped that beyond the strong coupling region, there is a scaling region for extracting continuum information when the physical quantities become approximately constants. From the intermediate coupling till the weak coupling, the data from the the truncated eigenvalue equation method show nice scaling behavior, thus suggesting the correct long wavelength continuum limit (1) of the vacuum wave function (2).

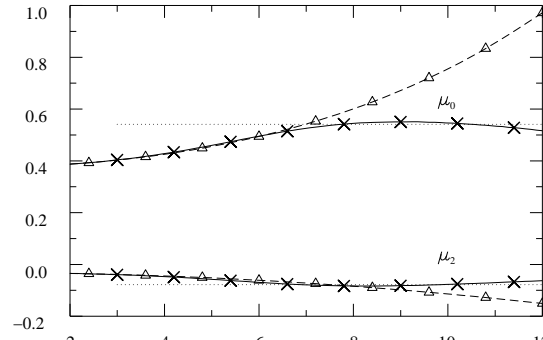


Figure 1: Coefficients in the vacuum wave function of QCD₃. Triangles: strong coupling expansion; Crosses: the third order calculation described in the text; The dot lines: mean values in the scaling region.

In [5], we present a possibly more efficient, named “inverse scheme”. Define the linear operations of derivation *Dev* and inverse *Inv* as

$$Dev[G] = \sum_l [E_l, [E_l, G]],$$

$$Inv[Dev[G]] = G. \quad (10)$$

Let us take some of the graphs in [4, 3] as examples,

$$Dev[G_1^\dagger] = \frac{16}{3}G_1^\dagger,$$

$$Inv[G_1^\dagger] = \frac{3}{16}G_1^\dagger,$$

$$Dev[G_{2,1}] = \frac{40}{3}G_{2,1} + 8G_1^\dagger. \quad (11)$$

Using (10) and (11), we have

$$Inv[G_{2,1}] = \frac{3}{40}(G_{2,1} - \frac{3}{2}G_1^\dagger). \quad (12)$$

In the inverse scheme, we choose the inverse of graphs $G_{n,j}$

$$G_{n,i}^I \propto Inv[G_{n,j}] \quad (13)$$

as independent graphs of order n . In general, $G_{n,i}^I$ is a linear combination of $G_{n,j}$ and lower order graphs. Up to the third order, the inverse of connected overlapping (c.o.) graphs $G_{n,j}$ (c.o.) in [3, 4] are

$$G_{2,1}^I = G_{2,1} - \frac{3}{2}G_1^\dagger,$$

$$G_{3,1}^I = G_{3,1} - G_{2,2},$$

$$G_{3,3}^I = G_{3,3} - \frac{9}{28}G_{2,5} + \frac{9}{28}G_{2,6},$$

$$G_{3,6}^I = G_{3,6} - \frac{1}{18}G_{3,5} - \frac{41}{99}G_{2,4} + \frac{227}{396}G_{2,3}. \quad (14)$$

We observe that in the inverse scheme, the independent operators $G_{n,i}^I$ are given by $G_{n,j}$ with subtraction of lower order graphs. (Actually there is alternation in sign in the lower order graphs in (14), but the dominant ones are subtractions). Such a subtraction may further reduce the overlapping of higher order graphs with lower order ones in the weak coupling region. Therefore, we expect that the inverse scheme may be superior over the other schemes.

Whereas our goal is to apply this method to QCD in 4 dimensions (in progress), we would like to demonstrate how the inverse scheme works in an interesting and relevant but less complicated theory: QCD_3 , the $3D$ $\text{SU}(3)$ gauge model. This reduces a theory to a super-renormalizable one, since the renormalization requirements amounts to dimensional analysis. In the weak coupling region (for large $\beta = 6/g^2$), because the renormalized charge e and the bare coupling are related by $g^2 = e^2 a$, dimensional analysis tells us that the dimensionless masses aM_{JPC} should scale as

$$\frac{aM_{JPC}}{g^2} \rightarrow \frac{M_{JPC}}{e^2} \approx \text{const.}, \quad (15)$$

from which the physical glueball masses M_{JPC} are obtained.

Figure 2: Glueball masses in QCD_3 indicated by crosses. The dot lines: mean values in the scaling region; Dash lines: strong coupling expansion; Triangles: results from a connected scheme.

The third order results for aM_{0++}/g^2 and aM_{0--}/g^2 are shown in Fig. 2 by crosses. For comparison, the results [4] using the old classification scheme (triangles) truncated up to the same order and those from the strong coupling expansion (dash lines) are also included in the figure. One sees clearly the advantage of the inverse scheme. While the mean values from different schemes are consistent, the scaling window for aM_{0++}/g^2 from the old scheme is $\beta \in [5, 8]$, and that from the inverse scheme is greatly widen and extended to much weaker coupling $\beta \approx 12$. The mean values for the masses extracted in the scaling region are

$$\begin{aligned} \frac{M_{0++}}{e^2} &\approx 2.0923 \pm 0.0334, \\ \frac{M_{0--}}{e^2} &\approx 3.7077 \pm 0.0280. \end{aligned} \quad (16)$$

In this paper, we discuss only the results for QCD_3 . The results of $3D - U(1)$, and $SU(2)$ gauge theories and $2D - \sigma$ model have been presented in [1, 2, 8] and summarized in [11]. Even at low orders, clear scaling windows for the physical quantities in all cases have been established, where the results are in perfect agreement with the Monte Carlo data [6, 9] (they have data only for $3D$ $SU(2)$). Extension to 3+1 dimensional nonabelian gauge theories is in progress.

To ensure that the results occur at their correct values, efforts have to be made in doing higher order calculations. In the applications to $3D - U(1)$ and $2D - \sigma$ models [10, 11], the convergence has been confirmed. In conclusion, the method is hopeful to be developed into an efficient systematic approach to extracting the continuum physics.

QZC and SHG are supported by Institute of Higher Education, and XQL is sponsored by DESY. We would like to thank H. Arisue, P.F. Cai, X.Y. Fang, C. Hamer, L. Li, J.M. Liu, D. Schütte, and W.H. Zheng for useful discussions.

References

- [1] S.H. Guo, Q.Z. Chen, and L. Li, Phys. Rev. D**49** (1994) 507.
- [2] Q.Z. Chen, S.H. Guo, W.H. Zheng, and X.Y. Fang, Phys. Rev. D**50** (1994) 3564.
- [3] Q.Z. Chen, X.Q. Luo, and S.H. Guo, Phys. Lett. B**341** (1995) 349.
- [4] Q.Z. Chen, X.Q. Luo, S.H. Guo and X.Y. Fang, Phys. Lett. B**348** (1995) 560.
- [5] Q.Z. Chen, X.Q. Luo, and S.H. Guo, **HLRZ-95-10**.
- [6] H. Arisue, Phys. Lett. B**280** (1992) 85.
- [7] J. Greensite, Nucl. Phys. B**166** (1980) 113.
- [8] S.H. Guo, Q.Z. Chen, X.Y. Fang and P.F. Cai, Zhongshan University Preprint.
- [9] M. Teper, Nucl. Phys. B(Proc. Suppl.) **30** (1993) 529.
- [10] X.Y. Fang, J.M. Liu, and S.H. Guo, Zhongshan University Preprint.
- [11] S.H. Guo, Q.Z. Chen, X. Fang, J. Liu, X.Q. Luo, and W. Zheng, these proceedings.

